Fuel 427 (2027) 139644

Contents lists available at ScienceDirect

Fuel

journal homepage: www.elsevier.com/locate/fuel

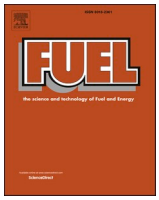

Full Length Article

Resolving rock eval limitations in overmature source rocks using high temperature pyrolysis

Xiaowei Zheng [a,b], Fujie Jiang [a,b,*], Hamed Sanei [c], Yutong Jiang [a,b], Qi He [a,b], Lorenz Schwark [d,**]

[a] National Key Laboratory of Petroleum Resources and Engineering, China University of Petroleum, Beijing 102249, China
[b] College of Geosciences, China University of Petroleum, Beijing 102249, China
[c] Lithospheric Organic Carbon (LOC) Group, Department of Geoscience, Aarhus University, 8000, Denmark
[d] Department of Geoscience, Kiel University, Kiel, Germany

ARTICLE INFO

Keywords:
Pyrolysis
Tmax
Hydrocarbon generation
Rock-Eval
Organic geochemistry

ABSTRACT

As unconventional hydrocarbon exploration increasingly targets deeply buried, highly mature source rocks, there is a growing need to accurately characterize organic matter exposed to extreme thermal conditions. A key analytical challenge in such systems is the reliable determination of total organic carbon (TOC), thermal maturity (Tmax), and hydrocarbon generation potential (S_2 and Hydrogen Index, HI) using standard Rock-Eval pyrolysis. In overmature samples, the conventional upper pyrolysis temperature of 650 °C is insufficient to fully evolve the S_2 peak, resulting in underestimated S_2 and TOC values and unreliable Tmax determinations. To overcome this limitation, this study introduces a modified extended temperature programmed pyrolysis protocol that extending the final temperature to 850 °C on a series of synthetically matured shale samples produced by confined-pressure hydrous pyrolysis across a range of thermal maturities. The results show that this approach enables complete S_2 evolution where conventional Rock–Eval analysis fails to resolve the hydrocarbon generation signal. The resulting S_2 pyrograms exhibit a bimodal distribution, with the first peak corresponding to residual kerogen and the second to pyrobitumen formation. Systematic evolution of the second peak yields robust Tmax values show a strong linear relationship with thermal maturity (Tmax = 95.17 EASY%Ro + 345.96), indicating that pyrobitumen serves as a reliable proxy for advanced thermal maturity. These results show that standard Rock-Eval protocols can significantly underestimate TOC and misrepresent maturity in overmature source rocks, whereas high-temperature programmed pyrolysis extends the applicability of pyrolysis-based geochemical parameters into the overmature domain. By enabling more accurate characterization of highly evolved organic matter, this method provides a practical and improved geochemical foundation for basin modeling and thermal simulation studies, addressing a critical gap in the evaluation of overmature petroleum systems.

1. Introduction

The accelerating global transition toward unconventional hydrocarbon resources has placed increasing emphasis on the accurate characterization of organic matter in deeply buried, thermally mature to overmature sedimentary successions [1,2]. As exploration targets extend into basins that have experienced complex thermal histories, the ability to robustly assess key geochemical parameters, like organic richness, hydrocarbon generation potential, and thermal maturity, becomes critical for refining basin models, and optimizing resource assessment [3]. Therefore, analytical methods that enable reliable evaluation of organic matter across the full thermal maturity spectrum are essential not only for petroleum geoscientists but also for basin modelers, reservoir engineers, and exploration experts.

The study of organic matter evolution through pyrolysis, particularly using Rock-Eval 6 analysis, is a cornerstone of geochemistry for rapid evaluating hydrocarbon potential in sedimentary basins [4–6]. This analytical technique, pioneered by Espitalié et al. [7], quantifying the free (S1) and thermally cracked (S2) hydrocarbons, as well as carbon dioxide (S3) released during analysis, is especially vital for regional

* Corresponding author at: National Key Laboratory of Petroleum Resources and Engineering, China University of Petroleum, Beijing 102249, China.
** Corresponding author.
E-mail addresses: jiangfj@cup.edu.cn (F. Jiang), lorenz.schwark@ifg.uni-kiel.de (L. Schwark).

https://doi.org/10.1016/j.fuel.2026.139644
Received 10 February 2026; Received in revised form 3 April 2026; Accepted 21 April 2026
Available online 30 April 2026

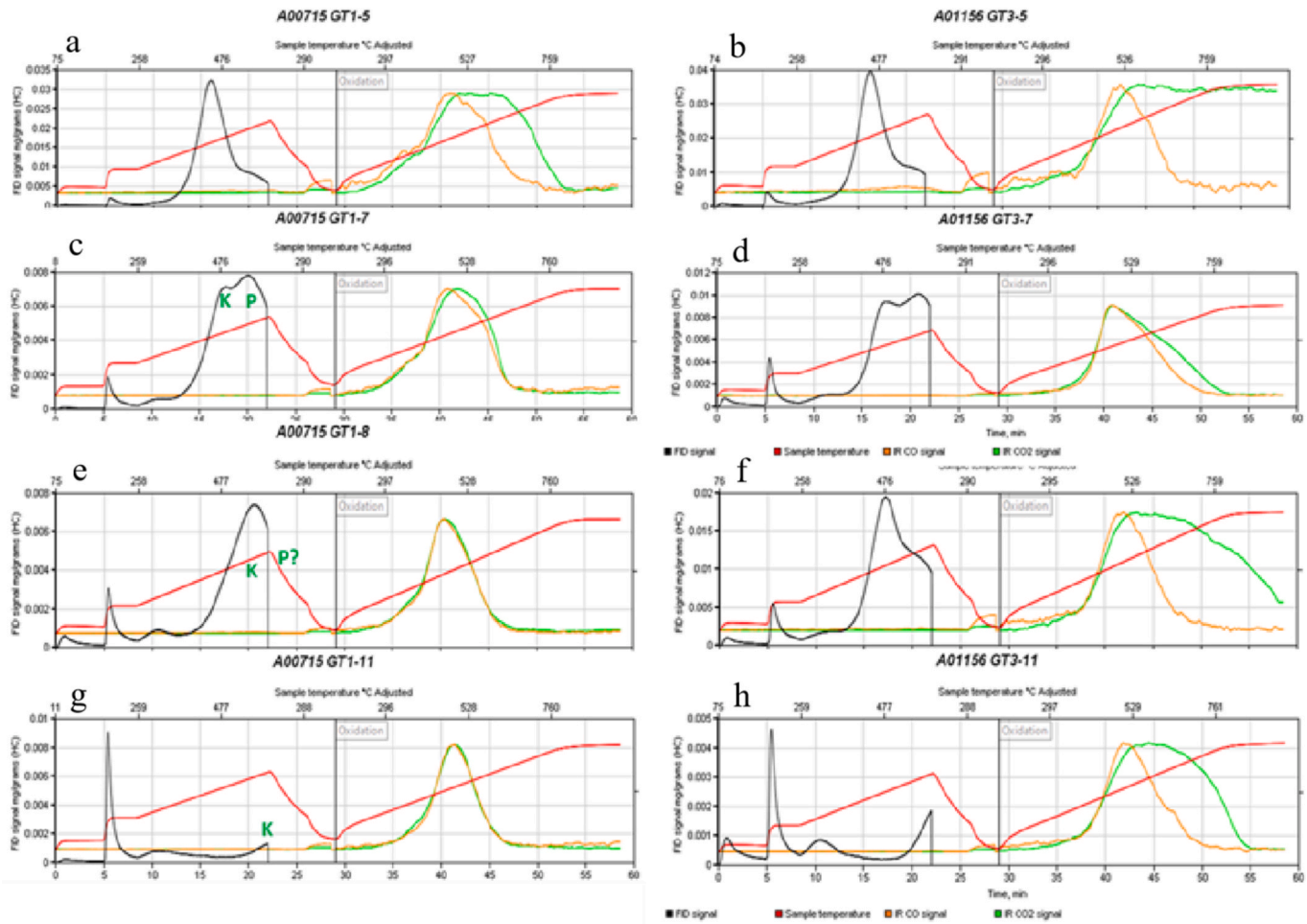

Fig. 1. The evolution trend of artificially matured samples showing the incomplete S2 pyrogram ends at 650 °C (a) and (b) with hydrous pyrolysis temperature of 350 °C, (c) and (d) with hydrous pyrolysis temperature of 390 °C, (e) and (f) with hydrous pyrolysis temperature of 400 °C, (g) and (h) with hydrous pyrolysis temperature of 470 °C).

screening and the characterization of unconventional shale reservoirs [8–10]. In Rock-Eval pyrolysis, Tmax corresponds to the temperature at which the S_2 peak attains its maximum and is widely applied as an empirical indicator of thermal maturity in petroleum source rocks. As thermal maturity increases, progressively more stable carbon structures require higher temperatures for cracking during programmed pyrolysis, producing higher Tmax values from the oil window into the gas window where pyrobitumen dominates [11–13].

However, the conventional analytical approaches often reach their limits in overmature systems [14], where the conventional Rock-Eval maximum pyrolysis temperature of 650 °C fails to fully evolve this material, limiting the reliability of Tmax and motivating the need for extended high-temperature protocols. In overmature source rocks, most hydrocarbons have already been generated and expelled, and the remaining organic matter has been transformed into refractory phases, primarily pyrobitumen or residual non-generative carbon [15]. These carbon forms contain little to no pyrolyzable hydrocarbons within the temperature range of conventional Rock-Eval analysis, resulting in a weak or absent S_2 signal and invalid Tmax values. [14,16–18].

Tmax reliability can be compromised in samples with very low S2 yields (typically below 0.2 mg HC/g rock), as the corresponding S2 peak becomes ill-defined, leading to inaccurate measurements [14,19]. Furthermore, contamination by migrated hydrocarbons or the presence of high-volatility bitumen can also suppress Tmax values [5,20].

The focus of traditional Rock-Eval 6 is predominantly on oil and gas generation stages and the pyrolysis temperature ends at 650 °C, hence the thermal parameters for determining the dimensions of oil window is conventionally defined as 435 °C ≤Tmax ≤470 °C [7,21], [4,17], which limited the implication of Tmax. Withe increasing shale gas sweet-spotting and identifying the limit of dry gas preservation, the maturity of overmature window also received a lot of attention. Although many works have reported about the limitation of traditional Rock-Eval 6, a systematic study that demonstrates how a complete S2 pyrogram can be obtained and how it provides a reliable evolution record for pyrobitumen in the overmature stage is still lacking. Therefore, this work conducted an extended-temperature pyrolysis with a higher ending temperature of 850 °C, which can generate a complete S2 pyrogram and hence a valid Tmax for heavily matured organic matter, to study the complete S2 pyrogram and to provide a reliable evolution record of the pyrobitumen generated at overmature stage. This will provide a comparative reference to study the heavily matured organic matter by a morphological study of the most convenient and widely applied pyrolysis pyrograms.

2. Samples and methodology

2.1. Sample information

An organic-rich lower Paleozoic Alum shale collected from Oland, Sweden was applied through a series of hydrous gold tube pyrolysis, followed by a extended programmed pyrolysis conducted on the solid residue. The TOC of the original sample is 9.55 wt%, which are tested in

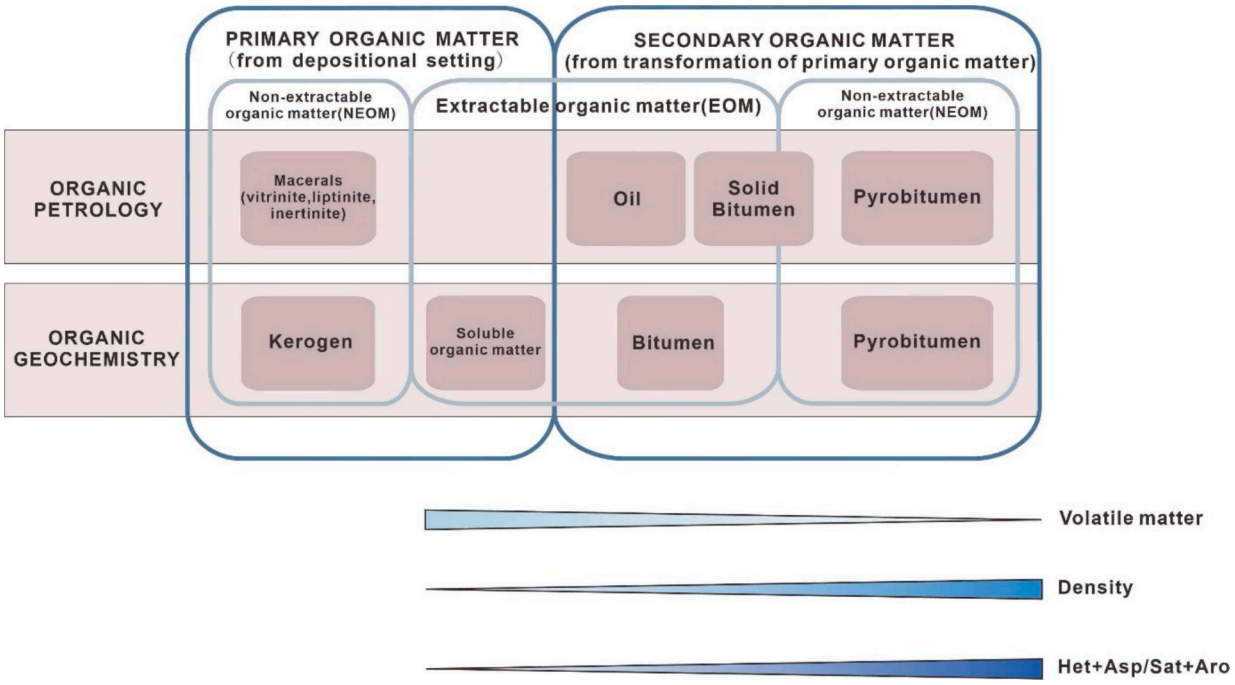

Fig. 2. Comparison of basic nomenclature of organic matter used by organic geochemists and organic petrologists (modified from Mastalerz et al., 2018). It compares the different terminologies of organic matter along thermal evolution between organic petrology and organic geochemistry based on stages and extractabilities.

Federal Institute for Geosciences and Natural Resources (BGR), Hannover, Germany. Its S1 is 1.28 mg/g, S2 is 49.47 mg/g, S3 is 0.4 mg/g and Tmax is 419 °C.

Two samples, Sample A00715 (Dju2008, 2.75 m, well Djupvik-2) and A001156 (DBH5060, 44.63 m, well Core601), have conducted confined hydrous pyrolysis (gold tube) experiment and generated two series of artificially matured samples with pyrolysis temperature of 275 °C, 300 °C, 325 °C, 350 °C, 370 °C, 390 °C, 400 °C, 415 °C, 440 °C, 470 °C, 500 °C, 550 °C, and 600 °C, corresponding to EASY%Ro [22] of 0.59%, 0.71%, 0.85%, 1.08%, 1.32%, 1.54%, 1.75%, 2.0%, 2.46%, 3.07%, 3.64%, 4.35%, and 4.67%, respectively. The geochemistry characteristics of the generated hydrocarbon of these samples were published in previous works [23,24]. The solid residue leftover were used for Standard Rock-Eval 6 pyrolysis in this work.

2.2. Confined hydrous pyrolysis (gold tube) experiment

The confined hydrous pyrolysis (gold tube) experiment was carried out at the National Key Laboratory of Petroleum Resources and Engineering, China University of Petroleum, Beijing. The process involved: 1) Crushed and sieved sample, in a size range of 1.5–2.5 mm, and deionized water with volume adjusted to 1:1, was added to gold tubes (40 mm long, 5.5 mm inner diameter, and 0.25 mm thick) and sealed under an argon atmosphere; 2) The pyrolysis was conducted at temperatures of 350 °C, 375 °C, 390 °C, 400 °C, 425 °C, 450 °C, 470 °C, 500 °C, 550 °C, and 600 °C, maintained isothermally for 72 h at a hydrostatic pressure of 50 MPa [25–27].

2.3. Standard Rock-Eval 6 pyrolysis

Total organic carbon (TOC) and Rock-Eval 6 pyrolysis parameters were determined using a HAWK analyzer (WILDCAT Technologies) following the standard Rock-Eval 6® methodology [7,28]. Analysis involved an initial pyrolysis stage (300 °C to 650 °C) under inert atmosphere to quantify free (S1) and kerogen-derived (S2) hydrocarbons, as well as CO_2 (S3) from oxygen-bearing compounds; thermal maturity was assessed via the Tmax parameter. Subsequently, the residual carbon was combusted in an oxidation oven (300 °C to 800 °C) to determine the non-generative organic carbon (300 °C to 650 °C) and mineral carbon (650 °C to 800 °C). The reported TOC (wt.%) represents the sum of organic carbon measured in both stages, pyrolyzable carbon (PC) and residual carbon (RC) [29,30]. Analytical precision, monitored using certified standards (WT2, IFP-160000) and duplicate analyses, was better than 5%.

2.4. A extended temperature programmed pyrolysis

A special extended programmed pyrolysis with an end temperature as high as 850 °C from the Department of Geoscience, Kiel University was adopted on the solid residues of the artificially matured samples after confined hydrous pyrolysis. Those run with a calibration for extended temperature, i.e., where the calibration standard WT2 provided by WILDCAT Technologies, has been used when running the standard up to 850 °C for calibration. From pyrolysis temperatures above 425 °C, the Tmax had to be determined manually, as the S2 intensity of the residual kerogen was very low.

3. Results and discussion

3.1. The evolution record of standard Rock-Eval 6 pyrogram

The pyrolysis data generated by Rock-Eval 6 analysis, specifically the characteristic pyrogram, undergoes a systematic and predictable evolution that serves as a fundamental proxy for the thermal maturity of sedimentary organic matter [31]. In immature sediments, the pyrogram is dominated by a prominent S2 peak from the thermal cracking of kerogen. Upon entering the oil window, free hydrocarbons (S1 peak) increases due to early generation, while S2 attains its maximum yield. With progressive maturation from peak oil to the wet gas window, the S2 peak area systematically depletes and Tmax increases, reflecting the depletion of labile kerogen components and the increasing thermal stability of the residual organic matrix [17,32]. However, there were rare works recorded the pyrogram evolution in overmature region.

As shown in Fig. 1, the Rock-Eval 6 pyrograms from two series of two

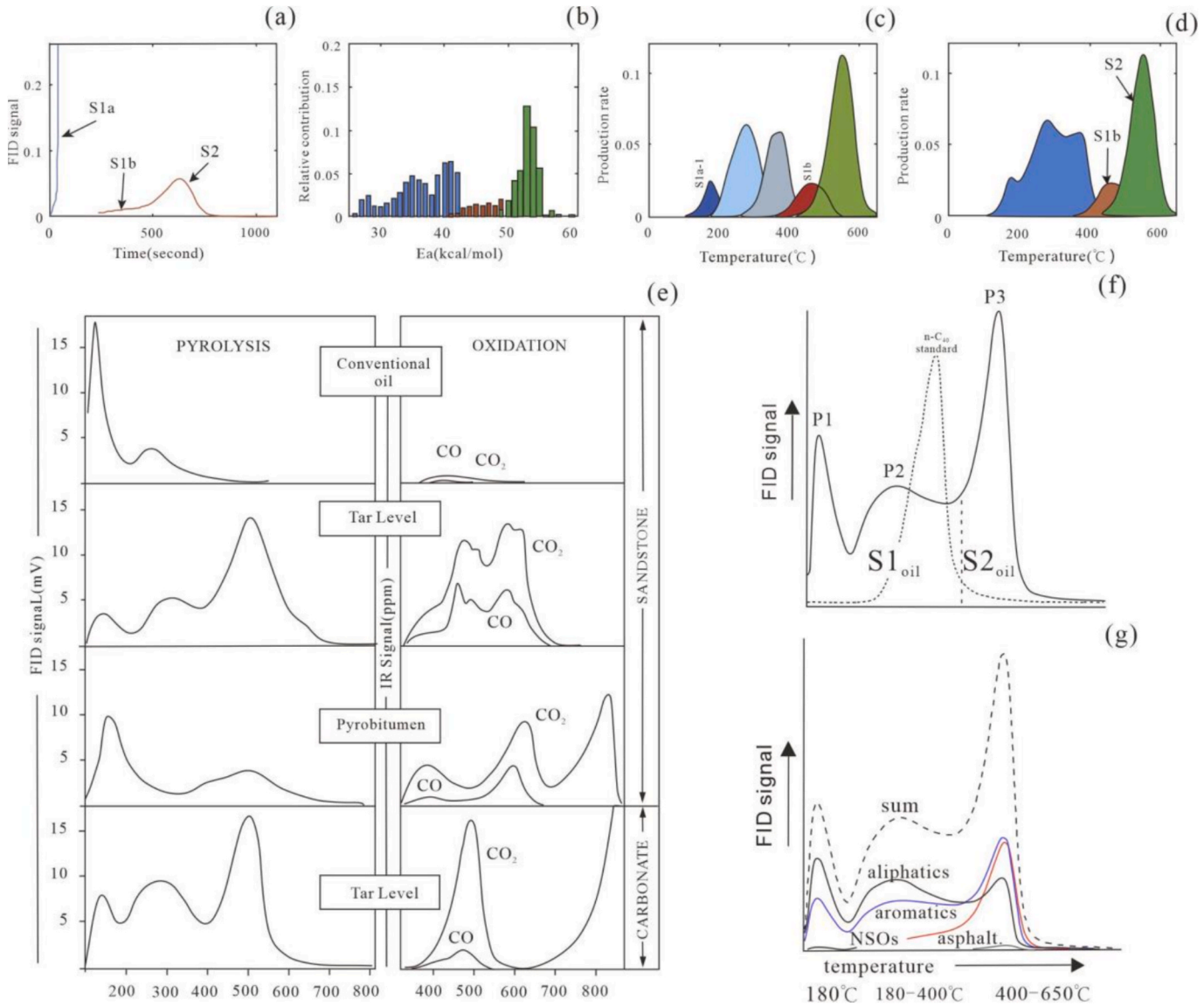

Fig. 3. General diagram showing the application of Rock-Eval to the study of reservoir rocks. (a) The common thematic diagrams showing FID pyrograms; (b) The activation energy distribution during pyrolysis; (c) Pyrogram dissection of organic matter pyrolysis showing thermal products grouped by different temperature ranges; (d) Products re-assembled groups (from [42]; (e) The pyrogram evolution of organic matter in pyrolysis and oxidation along maturation [28]; (f) Rock-Eval pyrograms of an early mature oil sample and the relationship between compound group fractions (Scheeder et al., 2020).

artificially matured samples showing the evolution trend of pyrogram and Tmax value along maturation, with the setting temperature of hydrous pyrolysis at 350 °C, 390 °C, 400 °C and 470 °C, shows that the shape of S2 change from mono-peak into bimodal peaks when the temperature change from 350 °C to 390 °C, with half of the right wing of the second peak being cut off at the ending pyrolysis temperature. After that, the whole S2 peak of sample generated at a hydrous pyrolysis temperature of 400 °C shift to the right ward and the second peak is completely cut off. After that, the S2 peaks are completely gone at the gold tube temperature of 470 °C. Hence, it shows clearly that the pyrobitumen generated from high maturity is not able to be pyrolyzed and leading to incomplete S2 (Fig. 1).

As S2 of Rock-Eval 6 is a geochemical composite, the heterogeneous nature of bitumen significantly complicates its interpretation, which is not exclusively representative of kerogen but a composite of multiple organic matter fractions. Such organic matter fractions can be classified as macerals, oil, solid bitumen and pyrobitumen in organic petrology; and kerogen, soluble organic matter, bitumen and pyrobitumen in organic geochemistry [33,34]. These fractions have distinct physical and chemical characteristics [35,36], which contains extractability, volatile matter content, density and the differing aliphatic, aromatics, NSOs and asphalts composition rate (Fig. 2). For instance, in the Vaca Muerta Formation, Bitumen I (easily extractable, aliphatic) and Bitumen II (released after demineralization, aromatic) are genetically distinct. Petrographically, Bitumen I correlates with fluorescent, oil-prone organic matter, while Bitumen II is linked to non-fluorescent amorphous material. This chemical heterogeneity means that the S2 peak can contain a substantial contribution from soluble but thermally stable bitumen, particularly at higher maturities, as demonstrated by hydrous pyrolysis experiments on the Posidonia Shale [34]. This is further corroborated in the Montney Formation, where an Extended Slow Heating Rock-Eval 6 cycle successfully separates a pore-coating, fluid-like hydrocarbon residue (S2aESH) from a pore-filling, solid bitumen fraction (S2bESH) [37]. Previous work on hydrous pyrolysis of Lower Toarcian Posidonia shale core plugs observed the generation of a soluble "thermally stable bitumen" that contributes to the S2 peak, marking an intermediate stage [38]. Therefore, the S2 peak in mature shales represents a mix of genuine kerogen and refractory, pore-filling bitumen,

Table 1
Summary of the extended pyrolysis results from a series of artificial matured samples after hydrous pyrolysis. Both non-extracted samples and samples after extracted were tested and documented.

Sample ID	Hy-Py Temperature	S1	S2	S3	TOC	Tmax (manual)	Tmax (auto)	HI	OI	GC	NGC	Comment
HT-PyB-350	350	3.67	9.84	0.73	8.22	449	449	119	8	1.42	6.8	**as received**
HT-Py Alum 350	350	2.58	9.13	1.17	7.83	452	452	116	14	1.25	6.58	**as received**
goldtube Py 350	350	0.04	8.07	0.31	6.52	452	452	123	4	0.75	5.76	**extracted**
HT-PyB-375	375	4.50	7.61	0.92	8.89	461	461	85	10	1.3	7.59	**as received**
HT-Py Alum 375	375	4.74	7.90	0.82	9.32	463	463	84	8	1.37	7.95	**as received**
goldtube Py 375	375	0.05	4.99	0.18	6.91	467	467	72	2	0.48	6.43	**extracted**
HT-PyB-390	390	3.39	6.29	0.98	8.58	461	461	73	11	1.04	7.55	**as received**
HT-Py Alum 390	390	3.57	6.86	1.11	8.56	461	461	80	13	1.13	7.43	**as received**
goldtube Py 390	390	0.03	4.81	0.30	6.94	465	465	69	4	0.47	6.48	**extracted**
HT-PyB-400	400	2.43	3.07	0.86	8.11	565	565	37	10	0.76	7.34	**as received**
HT-Py Alum 400	400	2.53	3.35	0.88	8.74	567	567	38	10	0.77	7.97	**as received**
goldtube Py 400	400	0.08	2.56	0.23	6.75	572	572	37	3	0.28	6.47	**extracted**
HT-PyB-425	425	1.90	2.25	0.66	8.28	586	586	27	7	0.62	7.66	**as received**
HT-Py Alum 425	425	1.98	2.66	0.62	9.05	581	581	29	6	0.6	8.45	**as received**
goldtube Py 425	425	0.08	1.84	0.25	7.15	589	589	25	3	0.21	6.94	**extracted**
goldtube 450C	450	0.30	2.20	0.17	7.09	593	589	31	2	0.25	6.84	**extracted**
HT-PyB-470	470	1.97	1.34	0.60	8.74		329	15	6	0.53	8.21	**as received**
HT-Py Alum 470	470	2.03	1.42	0.70	9.21		327	15	7	0.53	8.68	**as received**
goldtube Py 470	470	0.15	1.17	0.33	6.87	629	330	16	4	0.15	6.72	**extracted**
HT-PyB-500	500	1.72	1.20	0.92	9.55		326	12	9	0.5	9.05	**as received**
HT-Py Alum 500	500	1.70	1.12	0.76	9.17		328	12	8	0.41	8.76	**as received**
goldtube Py 500	500	0.17	0.86	0.23	7.28	671	357	11	3	0.13	7.14	**extracted**
HT-PyB-550	550	0.67	0.54	1.07	8.92		296	6	12	0.26	8.65	**as received**
HT-Py Alum 550	550	0.71	0.54	1.04	8.51		295	6	12	0.24	8.27	**as received**
goldtube 550C	550	0.36	0.74	0.44	7.36	718	344	10	5	0.16	7.2	**extracted**
HT-PyB-600	600	0.30	0.23	1.19	7.40		317	3	16	0.18	7.23	**as received**
HT-Py Alum 600	600	0.32	0.22	1.20	8.15		323	2	14	0.22	7.93	**as received**
goldtube Py 600	600	0.04	0.11	0.23	6.54	815	332	1	3	0.06	6.48	**extracted**

(HI:Hydrogen Index; HI: Oxygen Index; GC: Generative Carbon; NGC: Non-genarative Carbon).

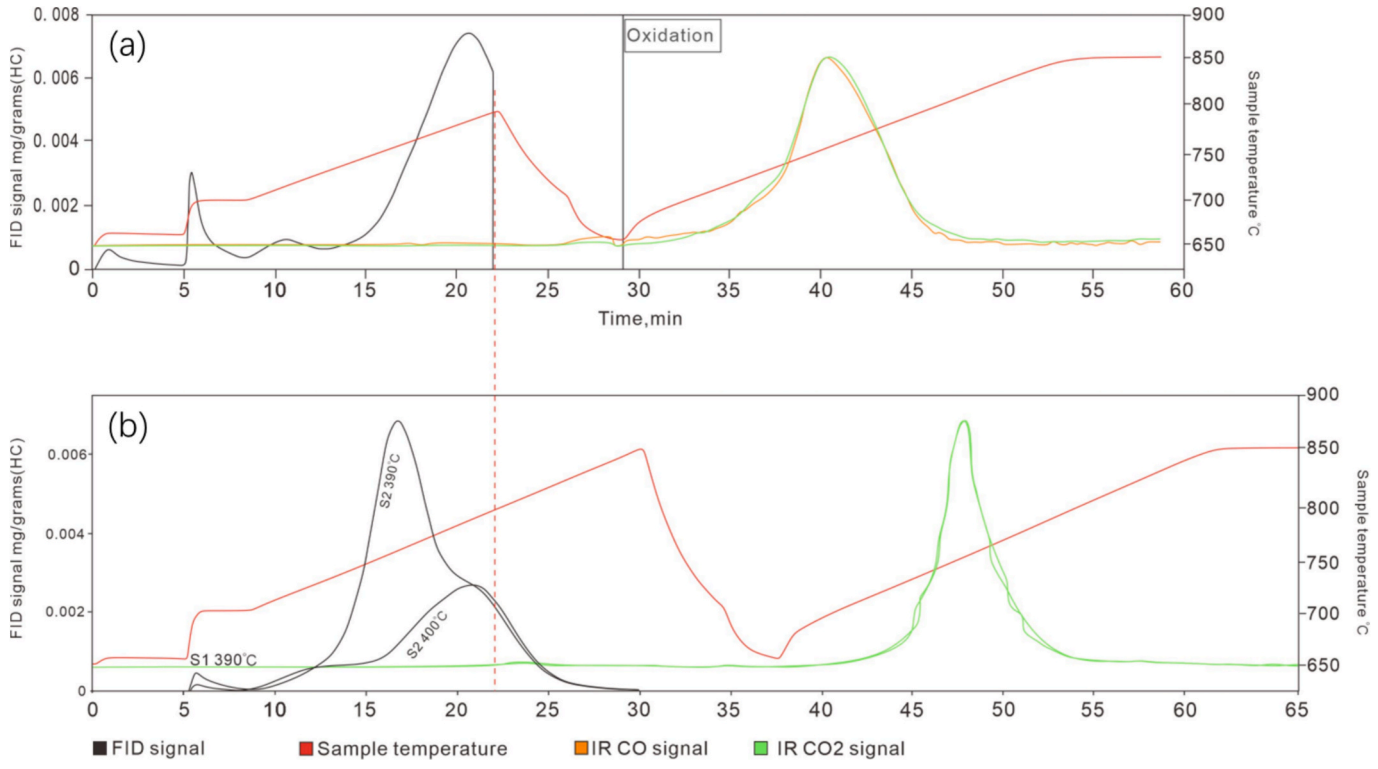

Fig. 4. The comparison of the pyrogram between the sample analyzed by standard Rock-Eval and the extended temperature programmed pyrolysis.

the latter of which can artificially elevate perceived hydrocarbon potential while simultaneously impairing reservoir porosity and fluid flow. The deconvolution of a complex S2 peak shape necessitating advanced pyrolysis protocols or complementary extraction to deconvolute these fractions for accurate assessment of hydrocarbon mobility and remaining generative capacity.

Many comprehensive analysis of the evolution of the Rock-Eval 6 pyrogram provide the record of the chemical composition of organic

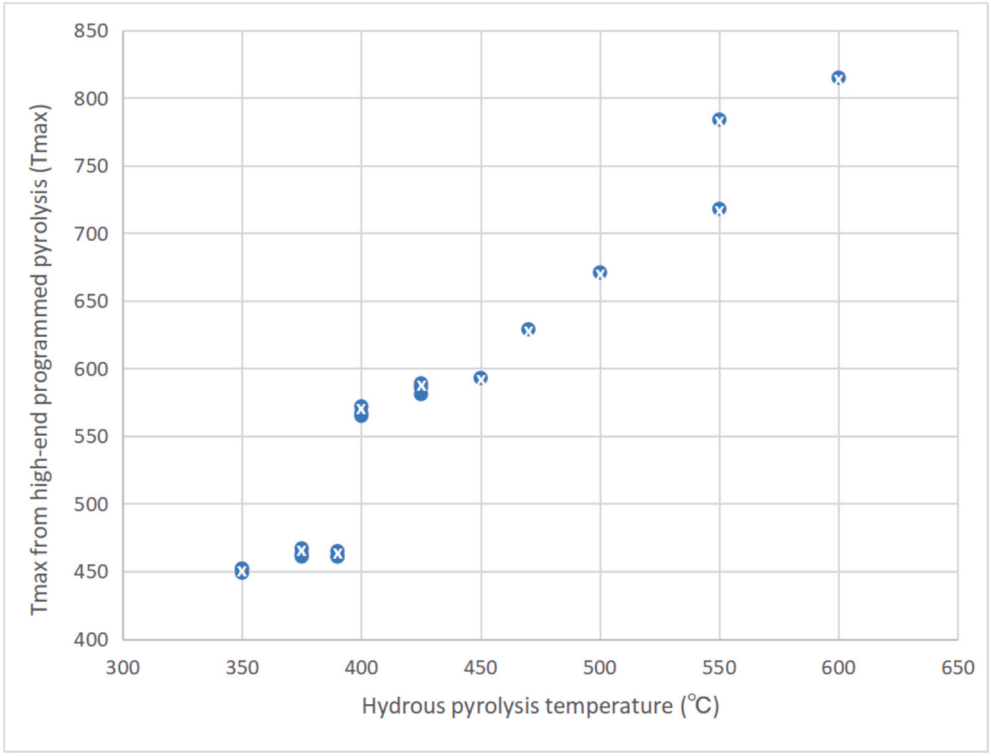

Fig. 5. The relationship between Tmax from extended temperature programmed pyrolysis and the hydrous pyrolysis temperature. It reveals three regression lines separated by two inflection points, marking the onset of pyrobitumen formation at 400 °C and the transition to the inertinization phase with advanced aromatization and condensation above 550 °C.

matter, and revealed that the morphological characteristics of S2 pyrogram serves as an integrated, chemically significant record of both organic matter type and its maturity [39–41], like the differing aliphatic, aromatics, NSOs and asphalts composition rate influences the S2 pyrogram shape (Fig. 3).

3.2. The results of extended-temperature programmed pyrolysis

Results of the extended-temperature programmed pyrolysis are recorded in Table 1, of which both non-extracted samples and samples after extracted were tested. Some of the non-extracted samples have been tested twice and both of the data were shown. Fig. 4 shows the pyrogram comparison of the standard pyrolysis ending at 650 °C (Fig. 4a) and the extended-temperature programmed pyrolysis with an ending temperature of 850 °C applied in this work (Fig. 4b). Different from the S2 peak with the right wing being cut off in the standard Rock-Eval 6, a complete S2 pyrogram can be formed and clearly deconvoluted in the extended-temperature programmed pyrolysis, and hence a valid Tmax can be generated. For pyrolysis temperatures exceeding 425 °C, Tmax was determined manually due to the low S2 intensity of the residual kerogen. The S2 traces exhibited a bimodal shape for samples subjected to pyrolysis above 400 °C, with an additional peak occurring at lower temperatures (around 375–400 °C), which may be attributed to residual bitumen rather than pyrobitumen. Hence, the beginning of the pyrobitumen formation could be detected by the changing shape of the pyrogram.

After manually obtained the Tmax value of over-mature samples, there show three regression relationships with two inflection points between Pyrolysis Temperature (Py-Temp) and the Tmax values (Fig. 5). The first inflection point starts at 400 °C, where the formation of pyrobitumen starts. As the hydrous pyrolysis temperature reaching above 550 °C, samples reach the inertinization phase, where molecules start high level of aromatization and condensation. This phenomenon was also reported in the study of biochar [43,44]. These maturities in artificial maturation can only be reached by very high-end gold tube pyrolysis (>3%Ro) and not by the frequently applied hydrous pyrolysis, however, showing potential reference value with the growing interest in high-end mature organic matter.

Hence, the linear regression between Tmax generated from the extended pyrolysis and EASY%Ro showed an equation of: Tmax = 95.17 EASY%Ro + 345.96 (R^2: 0.93), which extended the application area into high-end maturity region. The relationships between Tmax generated from Rock-Eval2, Rock-Eval6 and the extended temperature programmed pyrolysis v.s VRo were also compared, with the transferring equation from previous works reviewed in Fig. 6. It shows clearly that the three rates keep the same until VRo of 2.4%, which become divergent afterwards. The rate of Tmax from Rock-Eval2 and Rock-Eval 6 between VRo reach a pleateu, among which the rate of Tmax from Rock-Eval6 between VRo is higher than that between Tmax from Rock-Eval 2. This illustrate that Rock-Eval2 and Rock-Eval6 become invalid of telling the thermal maturity of overmature sample (EASY%Ro > 2.4%). Therefore, the extended temperature programmed pyrolysis extends the application region of Tmax into the thermal maturity it failed before.

3.3. Organic carbon and hydrous pyrolysis temperature

As shown in Fig. 7, there is a systematic difference between extracted and unextracted samples. The TOC evolution trend of gradual increase firstly and reverse after a pyrolysis temperature of 500 °C (VRo: 1.25%). This deviates from the conventional model of hydrocarbon generation via side-chain cracking from kerogen during thermal maturation [16,45], however, demonstrated an increase of the remaining organic carbon after high maturity level. This could be mostly attributed from the rapid increase of non-generative carbon (dead carbon) in high maturity. When heating under pyrolysis atmosphere (He) up to 850 °C, more organic matter is pyrolyzed than under maximum 650 °C. This small amount of additional pyrolyzate is captured in the S2 peak as hydrocarbons.

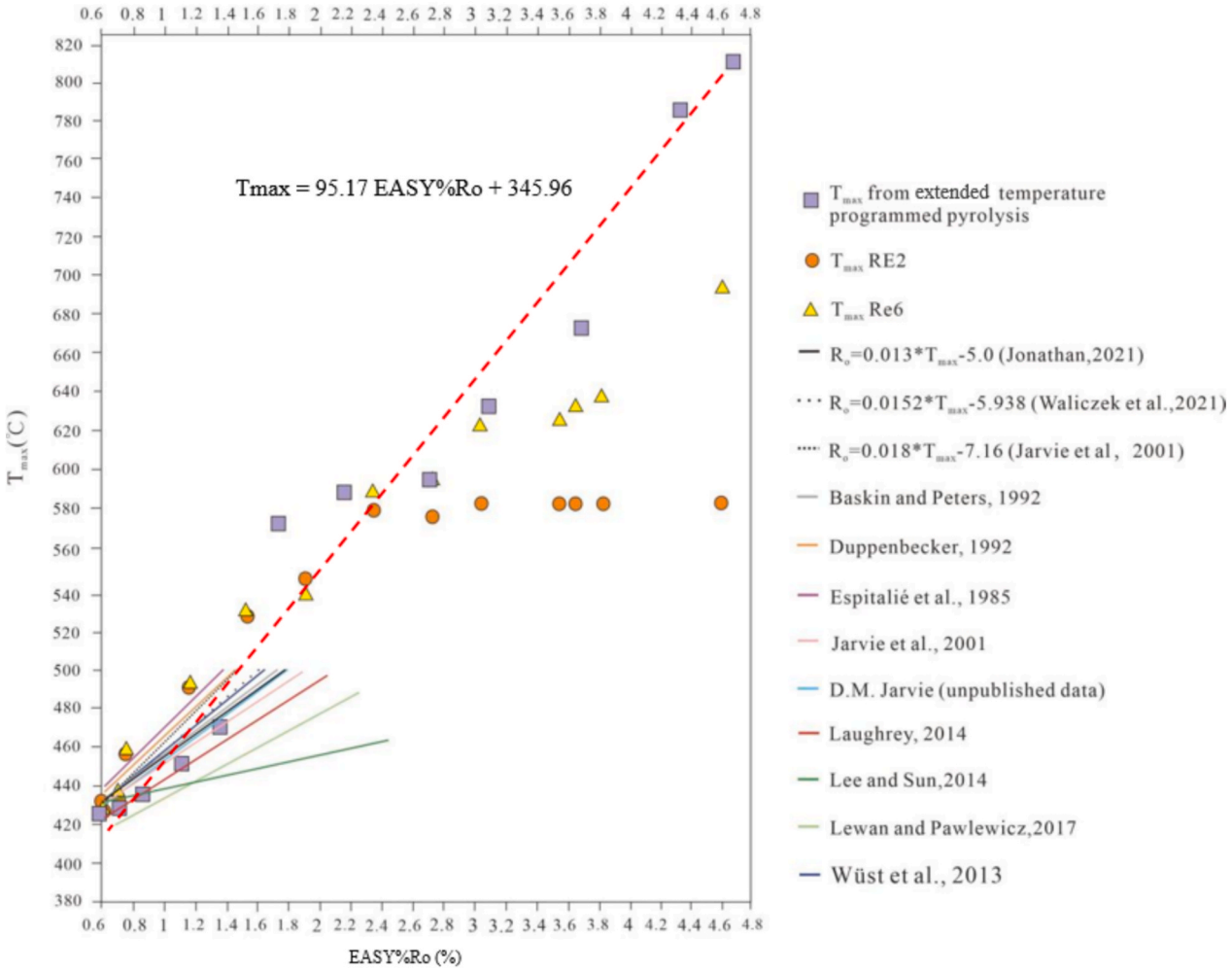

Fig. 6. The correlation between Tmax and Ro from extended pyrolysis (red dash line), Rock-Eval 6 and Rock-Eval 2 on a series of samples covering different thermal maturities in this work and a review of previous works of equation between Tmax and Ro (Espitalie et al., 1985; Baskin and Peters, 1992; Duppenbecker, 1992; Jarvie et al., 2001; Wust et al., 2013; Laughrey, 2014; Lee and Sun, 2014; Lewan and Pawlewicz, 2017). (For interpretation of the references to colour in this figure legend, the reader is referred to the web version of this article.)

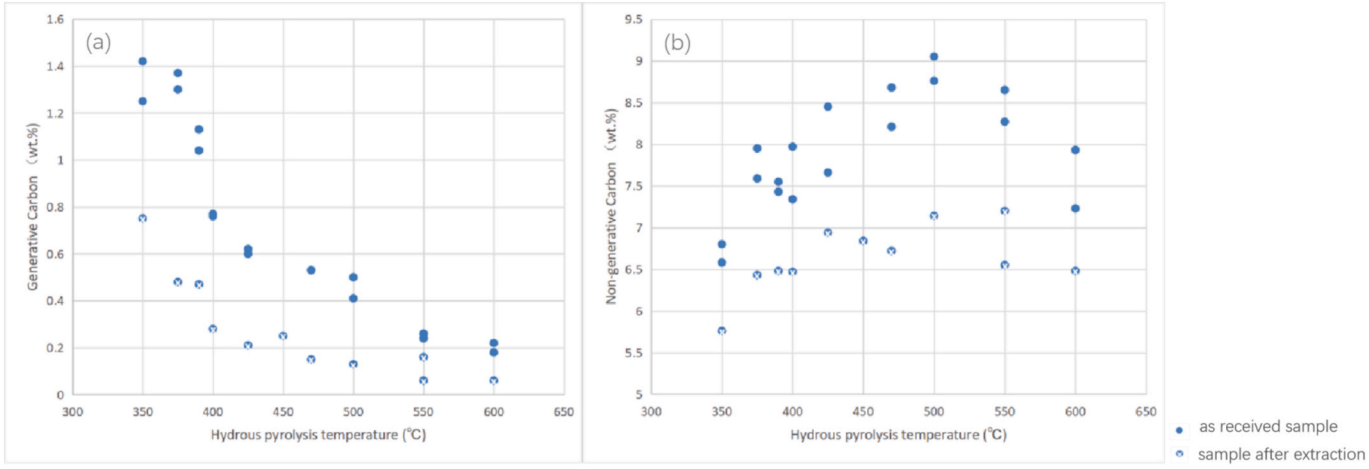

Fig. 7. The relationship between generative carbon and non-generative carbon from extended temperature programmed pyrolysis and the hydrous pyrolysis temperature. Although the amount of Generative carbon keeps decreasing, the amount of non-generative carbon increase until py-temperature of 500 °C and the trend reversed afterwards.

The evolution of generative carbon along pyrolysis temperatures are shown in Fig. 7a. Although the generative carbon keeps decrease, there is an obvious decreasing rate change of the relationship between generative carbon and pyrolysis temperatures after 425 °C, both in

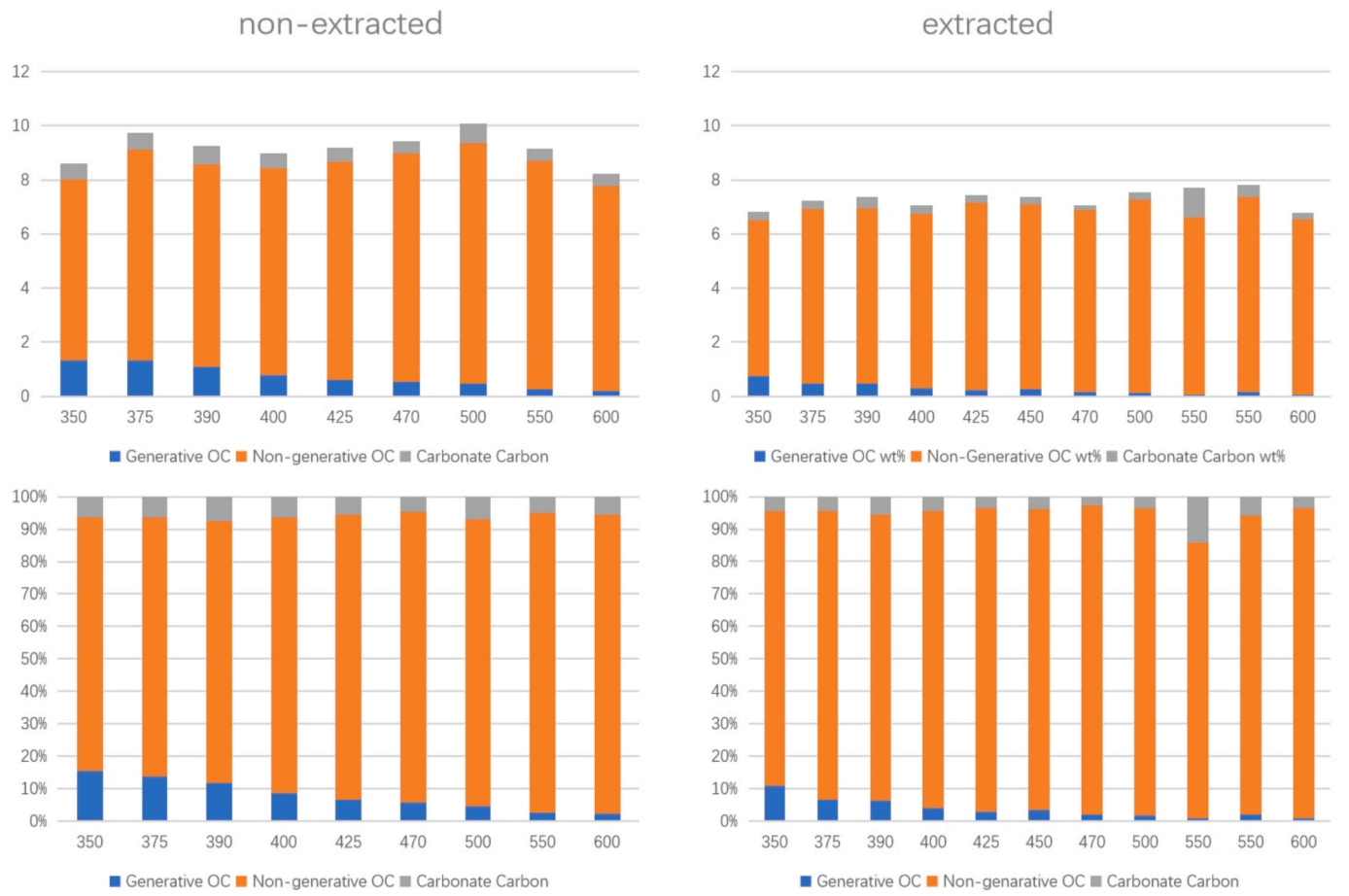

Fig. 8. Generative organic carbon, Non-generative organic carbon and carbonate carbon composition data generated from the extended temperature programmed pyrolysis of one series samples after hydrous pyrolysis (left column: as received, right coulmn: extracted).

samples before and after extraction. This demonstrated that the structure of the generative carbon changed greatly after 425 °C pyrolysis temperature (around VRo: 2.3%). These are in accordance with the predominance occurrence of pyrobitumen at this pyrolysis temperature [13,46]. What's more, the gap between extracted and non-extracted samples, which represents the generated bitumen, also started diminish after pyrolysis temperature of 425 °C. This illustrates the gas-window, where the rate of oil-cracking generated gas is higher than the rate of generated oil.

The relationship between non-generative carbon and Py-temperature is shown in Fig. 7b. The trend of non-extracted samples increase until py-temperature of 500 °C, which demonstrated the carbonization process of OM. After that, the trend turned into reversal and could be attributed from the break of aromatic carbon. The NGOC trend of extracted samples increase firstly until py-temperature of 425 °C and stay at a plateau after that, which could be hypothesized as the rate between carbonization and decomposition keep stable.

3.4. The underestimated TOC

If refractory organic matter (like pyrobitumen) is not cracked during standard pyrolysis (up to 650 °C), it remains in the crucible and should subsequently be oxidized and detected as RC (S4 peak) during the oxidation cycle (which typically goes up to 850 °C). Therefore, while the S2 peak is underestimated, the S2 + S4 should theoretically remain constant. However, Fig. 8 shows the organic carbon and carbonate carbon composition data generated from the extended temperature programmed pyrolysis. The TOC of extracted samples are 22% lower than the non-extracted samples, among which all the three types of carbon showing reduction from extraction. Therefore, part of the mineral carbon are attributed from extractable organic carbon.

Besides, the data from the standard Rock-Eval 6 of two series of artificially matured samples show that the content of mineral carbon start to increase at highly matured samples, among which the series of sample A001156 are more obvious than that of sample A00715 (Fig. 9). This could be explained as the standard oxidation cycle fails to recover the carbon in pyrobitumen. Such heavy pyrobitumen is not able to be oxidized below 600 °C, hence will be being misidentified as mineral carbon. Such difference between these two samples was hypothesized to be attributed from higher uranium content in sample A001156 (U: 227 ppm) than sample A00715 (U: 48 ppm). Many works reported that uranium content is positively correlated with the aromatization of both the free hydrocarbons and pyrolysates [47,48]. The enrichment of uranium within organic-bearing intervals facilitates intensive radiolysis, yielding a highly condensed, polycyclic aromatic network. This radiation-driven transformation often characterized by aromatic carbon fractions exceeding 70% significantly enhances the thermodynamic stability of the organic matter, rendering it refractory to standard thermal degradation. Such increased structural rigidity and bond resonance energy necessitate higher activation energies for combustion, manifested as a distinctive shift in the residual organic carbon (S4) oxidation peak toward temperatures exceeding 600 °C during Rock-Eval 6.

3.5. HI and hydrous pyrolysis temperature

As organic matter must be conjoined with hydrogen for significant hydrocarbon generation. The quantification of hydrogen content is

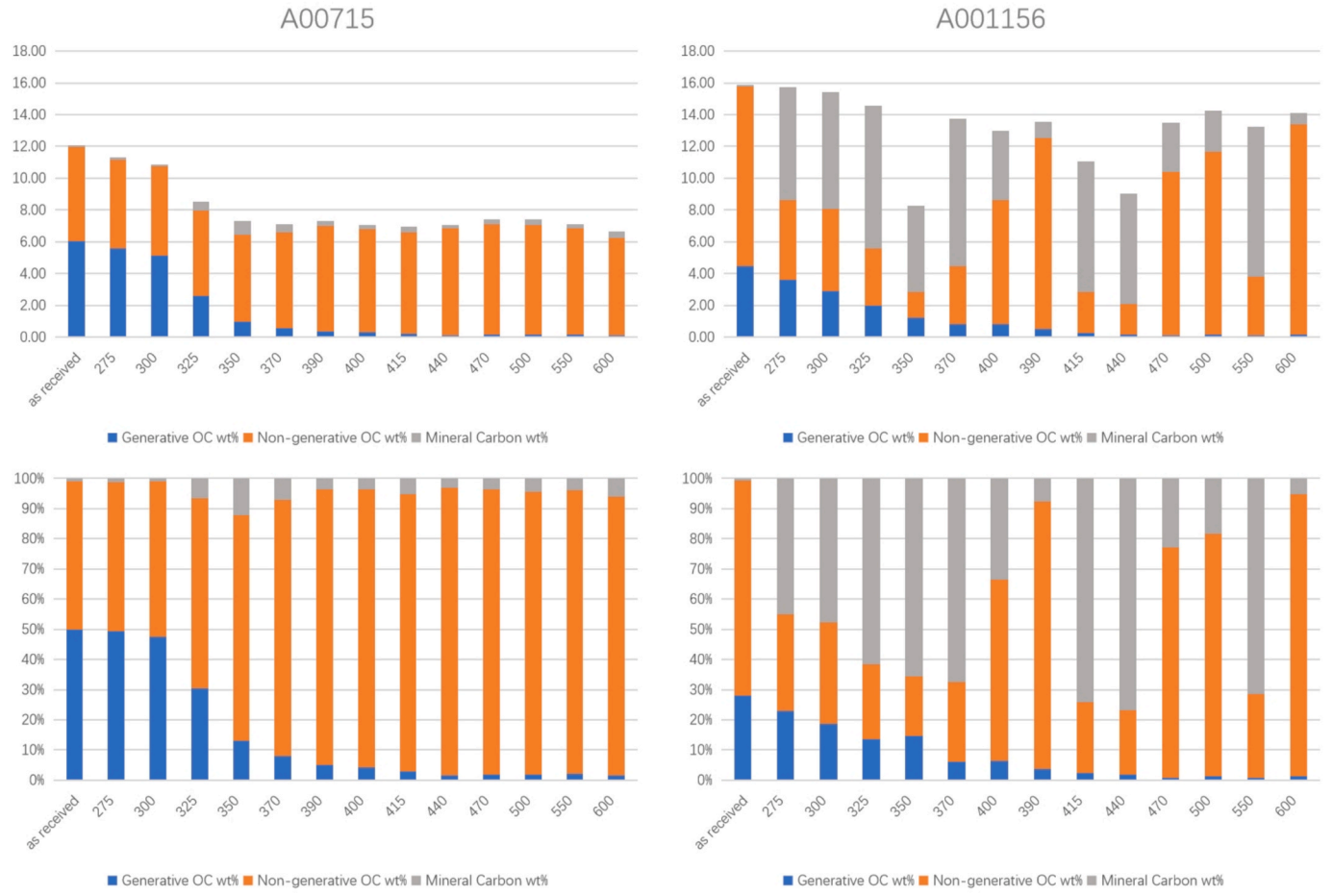

Fig. 9. Generative organic carbon, Non-generative organic carbon and carbonate carbon composition data generated from Rock-Eval 6 of two series samples after hydrous pyrolysis.

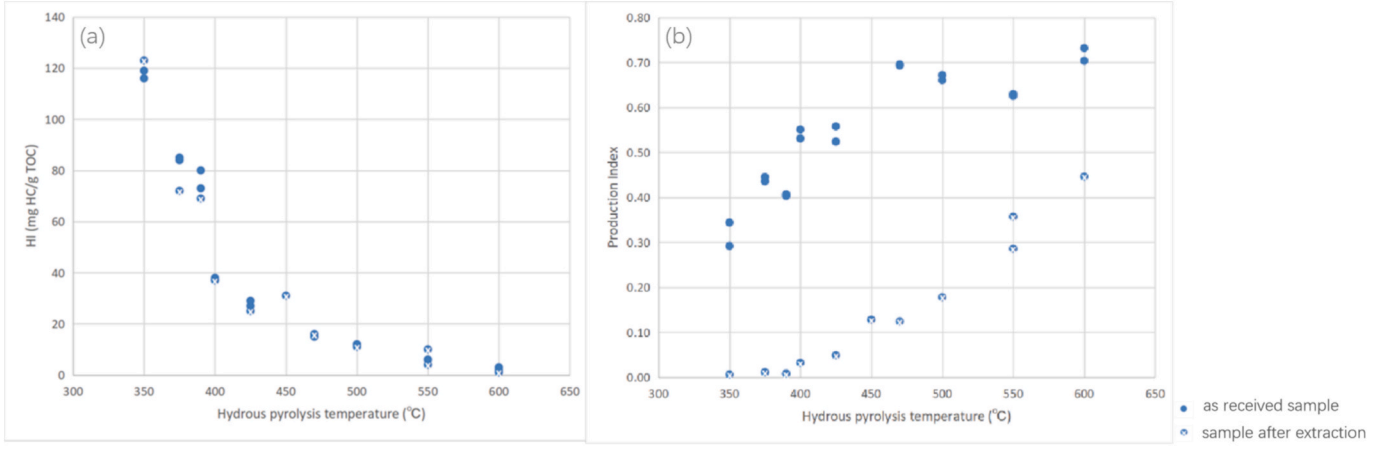

Fig. 10. The relationship between HI and PI from extended temperature programmed pyrolysis and the hydrous pyrolysis temperature. The hydrogen index keeps decreasing while the production index reaches its limit after 425 °C, marking the oil generation stage. The production index of as received samples reach a plateau above 450 °C could be explained as pyrobitumen formation during secondary hydrocarbon generation.

significant to measure the hydrocarbons formed during the thermal decomposition of organic matter in the sample, which can be showed by S2 (Espitalie et al., 1977) and hydrogen index (HI). The relationship between Py-temp vs. S2 and Py-temp vs. HI are shown in Fig. 10a. Both trends have a drastic decreases before pyrolysis temperature of 440 °C and become relatively flat after that. Therefore, the hydrocarbon generation potential mostly expires at pyrolysis temperature of 440 °C (VRo: 2.46%).

The relationship between production index and pyrolysis temperatures of the samples before and after extraction also show clear difference (Fig. 10b). It also shows that the production index of a closed system reached the limit after Py-temperature of 425 °C, which documented the oil generation and evolution process. As S1 in the after-extracted samples represents the pyrolyzable organic matter that are

not extractable, the increasing trend after 450 °C recorded the generation of pyrobitumen during the secondary hydrocarbon generation stage.

4. Conclusion

This work addressed the limitations of conventional Rock–Eval pyrolysis for assessing overmature source rocks by extending the programmed pyrolysis temperature to 850 °C. Our experimental results demonstrate that this extended protocol recovers the truncated S2 signal, enabling reliable determination of Tmax and TOC in samples where standard 650 °C runs fail. Such extended temperature programmed pyrolysis produced complete S2 pyrograms, which often showing bimodal and revealing a robust linear relationship between artificial hydrous maturation temperature and Tmax = 95.17 EASY%Ro + 345.96. A critical transition near 425–450 °C (approximately equivalent to Ro ~ 2.3–2.5%) is identified, marked by sharp declines in generative carbon and hydrogen index, alongside increases in non-generative carbon and pyrobitumen formation. These findings indicate that conventional Rock-Eval protocols can substantially underestimate TOC and misrepresent the thermal maturity of overmature source rocks. By extending the temperature range, the proposed method provides a practical means to extend reliable maturity and TOC assessment into the overmature domain. Collectively, our work fills a key gap in the literature by demonstrating that accurate reconstruction of original organic matter in high-maturity systems requires careful selection and calibration of the pyrolysis methodology. This improved approach thus offers a more robust basis for characterizing overmature organic matter, with important implications for the evaluation of petroleum systems that have experienced elevated thermal stress.

CRediT authorship contribution statement

Xiaowei Zheng: Writing – original draft, Project administration, Investigation, Data curation, Conceptualization. **Fujie Jiang:** Investigation, Funding acquisition. **Hamed Sanei:** Writing – review & editing, Validation, Supervision, Methodology, Formal analysis. **Yutong Jiang:** Visualization, Methodology. **Qi He:** Visualization, Methodology. **Lorenz Schwark:** Validation, Supervision, Methodology, Investigation, Formal analysis, Data curation, Conceptualization.

Declaration of competing interest

The authors declare the following financial interests/personal relationships which may be considered as potential competing interests: Xiaowei Zheng reports financial support was provided by National Natural Science Foundation of China. If there are other authors, they declare that they have no known competing financial interests or personal relationships that could have appeared to influence the work reported in this paper.

Acknowledgements

Xiaowei Zheng acknowledges the financial support of Start-up Funding from China University of Petroleum, Beijing (2462024BJRC007) and the National Natural Science Foundation of China (No. 42402149). This is a contribution to the project of Theory of Hydrocarbon Enrichment under Multi-Spheric Interactions of the Earth (Grant No. THEMSIE04010105).

Data availability

Data will be made available on request.

References

[1] Zou C, Zhai G, Wangm H, Li J, Wang Z, Wen Z, et al. Formation, distribution, potential and prediction of global conventional and unconventional hydrocarbon resources. Pet Explor Dev 2015;42(1):14–28.
[2] Jia C, Zheng M, Zhang Y. Some key issues on the unconventional petroleum systems. Pet Res 2016;1(2):113–22.
[3] Xiao W, Cao J, Luo B, Wang Y, Xiao D, Shi C, et al. Recovering original type and abundance of organic matter in spent source rocks: a review and advances in elemental proxies. AAPG Bull 2023;107(2):243–81.
[4] Behar F, Beaumont V, De Penteado B. Rock-eval 6 technology: performances and developments. Oil Gas Sci Technol 2001;56:111–34.
[5] Carvajal-Ortiz H, Gentzis T. Critical considerations when assessing hydrocarbon plays using Rock-Eval pyrolysis and organic petrology data: data quality revisited. Int J Coal Geol 2015;152:113–22.
[6] Sykes R, Snowdon LR. Guidelines for assessing the petroleum potential of coaly source rocks using Rock-Eval pyrolysis. Org Geochem 2002;33:1441–55.
[7] Espitalié J, Laporte JL, Madec M, Marquis F, Leplat P, Paulet J, et al. Méthode rapide de caractérisation des roches mètes, de leur potentiel pétrolier et de leur degré d'évolution. Rev De l'Inst Fr du Pétrole 1977;32:23–42.
[8] Dembicki H. Three common source rock evaluation errors made by geologists during prospect or play appraisals. AAPG Bull 2009;93:341–56.
[9] Hackley PC, Cardott BJ. Application of organic petrography in north American shale petroleum systems: a review. Int J Coal Geol 2016;163:8–51.
[10] Li M, Chen Z, Ma X, Cao T, Qian M, Jiang Q, et al. Shale oil resource potential and oil mobility characteristics of the Eocene-Oligocene Shahejie Formation, Jiyang Super-Depression, Bohai Bay Basin of China. Int J Coal Geol 2019.
[11] Nali M, Caccialanza G, Ghiselli C, Chiaramonte MA. Tmax of asphaltenes: a parameter for oil maturity assessment. Org Geochem 2000;31(12):1325–32.
[12] Reyes J, Jiang C, Lavoie D, Milovic M, Robinson R, Zhang S, et al. Determination of hydrocarbon generation and expulsion temperature of organic-rich Upper Ordovician shales from Hudson Bay and Foxe basins using modified hydrous pyrolysis, organic petrography, Rock-Eval and organic solvent extraction. Geological Survey of Canada, Open File 2016;8049:62.
[13] Chen J, Jia W, Yu C, Zhang X, Peng PA. Bound hydrocarbons and structure of pyrobitumen rapidly formed by asphaltene cracking: Implications for oil–source correlation. Org Geochem 2020;146:104053.
[14] Yang S, Horsfield B. Critical review of the uncertainty of Tmax in revealing the thermal maturity of organic matter in sedimentary rocks. Int J Coal Geol 2025;225.
[15] Sanei H. Genesis of solid bitumen. Scientific Reports. 2020 Sep 24;10(1):15595.
[16] Tissot BP, Welte DH. Kerogen: composition and classification. In: Petroleum Formation and Occurrence; 1984. p. 131–59.
[17] Peters KE. Guidelines for evaluating petroleum source rock using programmed pyrolysis. AAPG Bull 1986;70:318–29.
[18] Jarvie DM. Shale resource systems for oil and gas: part 1—shale-gas resource systems. AAPG Mem 2012:89–119.
[19] Peters KE, Walters CC, Mankiewicz PJ. Evaluation of kinetic uncertainty in numerical models of petroleum generation. AAPG Bull 2006;90:387–403.
[20] Katz BJ, Lin F. Consideration of the limitations of thermal maturity with respect to vitrinite reflectance, Tmax, and other proxies. AAPG Bull 2021;105:695–720.
[21] Espitalié J, Burrus J. Use of Tmax as a maturation index for different types of organic matter. Comparison with vitrinite reflectance. Thermal modelling in sedimentary basins 1986;11:475–96.
[22] Sweeney JJ, Burnham AK. Evaluation of a simple model of vitrinite reflectance based on chemical kinetics. AAPG Bull 1990;74:1559–70.
[23] Zheng X, Sanei H, Schovsbo NH, Luo Q, Wu J, Zhong N, et al. Role of zooclasts in the kerogen type and hydrocarbon potential of the lower Paleozoic Alum Shale. Int J Coal Geol 2021;248:103865.
[24] Zheng X, Schovsbo NH, Luo Q, Wu J, Zhong N, Goodarzi F, et al. Graptolite reflectance anomaly. Int. J Coal Geol 2022.
[25] Lewan MD. Evaluation of petroleum generation by hydrous pyrolysis experimentation. Phil Trans R Soc Lond A 1985;315(1531):123–34.
[26] Jin X, Wu J, Silva RC, Huang H, Zhang Z, Zhong N, et al. Alternate routes to sustainable energy recovery from fossil fuels reservoirs. Part 1. Investigation of high-temperature reactions between sulfur oxy anions and crude oil. Fuel 2021; 302:121050.
[27] Wu J, Qi W, Jiang FJ, Luo QY, Zhang CL, Hu HZ, et al. Influence of sulfate on the generation of bitumen components from kerogen decomposition during catagenesis. Pet Sci 2021;18:1611–8.
[28] Lafargue E, Marquis F, Pillot D. Rock-Eval 6 applications in hydrocarbon exploration, production, and soil contamination studies. Revue Inst Fr Pétrole 1998;53(4):421–37.
[29] Pillot D, Deville E, Prinzhofer A. Identification and quantification of carbonate species using Rock-Eval pyrolysis. Oil Gas Sci Technol – Rev IFP Energies nouvelles 2014;69(2):341–9.
[30] Romero-Sarmiento MF, Pillot D, Letort G, Lamoureux-Var V, Beaumont V, Huc AY, et al. New Rock-Eval method for characterization of unconventional shale resource systems. Oil Gas Sci Technol 2016;71(3):37.
[31] Espitalié J, Deroo G, Marquis F. La pyrolyse Rock-Eval® et ses applications; première partie. Rev De l'Institut Fr du Pétrole 1985;40:563–79.
[32] Shirokova V, Spasennykh M. Analytical modeling of kerogen maturation pathways: linking pyrolytic characteristics of source rocks (HI-Tmax) with kerogen thermal decomposition kinetics. Int J Coal Geol 2026:104963.
[33] Jacob H. Classification, structure, genesis and practical importance of natural solid oil bitumen ("migrabitumen"). Int J Coal Geol 1989;11(1):65–79.

[34] Małachowska A, Mastalerz M, Hampton L, Hupka J, Drobniak A. Origin of bitumen fractions in the Jurassic-early cretaceous Vaca Muerta Formation in Argentina: insights from organic petrography and geochemical techniques. Int J Coal Geol 2019;205:155–65.
[35] Carrie J, Sanei H, Stern G. Standardisation of Rock–Eval pyrolysis for the analysis of recent sediments and soils. Org Geochem 2012;46:38–53.
[36] Dang W, Zhang J, Tang X, Chen Q, Han S, Li Z, et al. Shale gas potential of lower Permian marine-continental transitional black shales in the Southern North China Basin, central China: Characterization of organic geochemistry. J Nat Gas Sci Eng 2016;28:639–50.
[37] Sanei H, Wood JM, Ardakani OH, Clarkson CR, Jiang C. Characterization of organic matter fractions in an unconventional tight gas siltstone reservoir. Int J Coal Geol 2015;150–151:296–305.
[38] Arysanto A, Burnaz L, Zheng T, Littke R. Geochemical and petrographic evaluation of hydrous pyrolysis experiments on core plugs of lower toarcian posidonia shale: comparison of artificial and natural thermal maturity series. Int J Coal Geol 2024; 284:30.
[39] Sebag D, Disnar JR, Guillet B, Di Giovanni C, Verrechia EP, Durand A. Monitoring organic matter dynamics in soil profiles by Rock-Eval® pyrolysis: bulk characterization and quantification of degradation. Eur J Soil Sci 2006;57:344–55.
[40] Copard Y, Di-Giovanni C, Martaud T, Albéric P, Olivier JE. Using Rock-Eval® 6 pyrolysis for tracking fossil organic carbon in modern environments: implications for the roles of erosion and weathering. Earth Surf Proc Land 2006;31:135–53.
[41] Jacob J, Delarue F, Copard Y, et al. Comparison between Rock-Eval and temperature-programmed pyrolysis/mass spectrometry for the analysis of environmental and geological samples. J Anal Appl Pyrol 2023;173:10.
[42] Li M, Chen Z, Qian M, Ma X, Jiang Q, Li Z, et al. What are in pyrolysis S1 peak and what are missed? Petroleum compositional characteristics revealed from programed pyrolysis and implications for shale oil mobility and resource potential. Int J Coal Geol 2020;217:103321.
[43] Petersen HI, Sanei H. The H/C molar ratio and its potential pitfalls for determining biochar's permanence. GCB Bioenergy 2025;17(6):e70049.
[44] Sanei H, Petersen HI, Chiaramonti D, Masek O. Evaluating the two-pool decay model for biochar carbon permanence. Biochar 2025;7(1):9.
[45] Behar F, Kressmann S, Rudkiewicz JL, Vandenbroucke M. Experimental simulation in a confined system and kinetic modelling of kerogen and oil cracking. Org Geochem 1992;19(1–3):173–89.
[46] Wu L, Liu S, Fang X, Wang P, Geng A. Formation of pyrobitumen from different types of crude oils and its significance: Insight from elemental composition analysis. Mar Pet Geol 2023;152:106227.
[47] Yang S, Schulz HM, Horsfield B, Schovsbo NH, Noah M, Panova E, et al. On the changing petroleum generation properties of Alum Shale over geological time caused by uranium irradiation. Geochim Cosmochim Acta 2018;229:20–35.
[48] Wang W, Liu C, Liu W, Wang X, Guo P, Wang J, et al. Dominant products and reactions during organic matter radiolysis: Implications for hydrocarbon generation of uranium-rich shales. Mar Pet Geol 2022;137:105497.